

Delivery of raft-associated, GPI-anchored proteins to the apical surface of polarized MDCK cells by a transcytotic pathway

Roman Polishchuk^{1,2}, Alessio Di Pentima² and Jennifer Lippincott-Schwartz^{1,3}

Epithelial cell polarity depends on mechanisms for targeting proteins to different plasma membrane domains. Here, we dissect the pathway for apical delivery of several raft-associated, glycosyl phosphatidylinositol (GPI)-anchored proteins in polarized MDCK cells using live-cell imaging and selective inhibition of apical or basolateral exocytosis. Rather than trafficking directly from the *trans*-Golgi network (TGN) to the apical plasma membrane as previously thought, the GPI-anchored proteins followed an indirect, transcytotic route. They first exited the TGN in membrane-bound carriers that also contained basolateral cargo, although the two cargoes were laterally segregated. The carriers were then targeted to and fused with a zone of lateral plasma membrane adjacent to tight junctions that is known to contain the exocyst. Thereafter, the GPI-anchored proteins, but not basolateral cargo, were rapidly internalized, together with endocytic tracer, into clathrin-free transport intermediates that transcytosed to the apical plasma membrane. Thus, apical sorting of these GPI-anchored proteins occurs at the plasma membrane, rather than at the TGN.

Epithelial cells have apical and basolateral plasma membrane domains with differing protein compositions and absorptive/secretory activities. Separated by tight junctions, the polarized domains utilize sophisticated sorting and trafficking machinery to be generated and maintained. As a result, newly synthesized proteins are transported to polarized surfaces by a direct or indirect route^{1–4}. In the direct pathway, TGN-derived carriers are targeted selectively to apical or basolateral domains³. In the indirect pathway, however, transport intermediates undergo transcytosis from one plasma membrane domain to another². Establishing which proteins are transported by each pathway is the subject of continuing investigations⁵.

Within each pathway, specific sorting machinery is essential. Apical sorting machinery recognizes signals that are found in either the trans-membrane domain or ectodomain of a protein. These include *N*- and *O*-linked glycans^{6,7}, as well as GPI- and transmembrane-anchors^{8,9}. Accumulating evidence suggests that these signals help sequester apical proteins into glycosphingolipid-cholesterol-rich domains, or ‘rafts’, found in the plasma membrane and the TGN⁹. The basolateral sorting machinery, however, recognizes signals found in the cytoplasmic tail of a protein^{10,11}. These signals interact with distinct molecular subunits of adaptor complexes, such as the μ 1B subunit of the adaptor protein 1 (AP-1) complex¹².

It is unclear at what transport step(s) the basolateral and apical sorting signals on proteins are recognized and acted on. Basolateral sorting machinery is found on both the TGN and endocytic membranes, and could therefore operate at either location^{12–14}. Similarly,

protein partitioning into lipid raft domains, which is important for some types of apical sorting, can occur at either the TGN or the cell surface^{9,15}, and when it occurs at the plasma membrane it can result in selective uptake of proteins^{16–18}. Live-cell imaging represents a promising approach for determining where these sorting events occur.

In non-polarized cells, live-cell imaging has revealed that newly synthesized apical and basolateral cargos cluster in the TGN into large domains that bud off as carriers^{19–23}, and that GPI-anchored proteins are laterally segregated from basolateral cargo in the TGN²⁰. Together with previous biochemical findings, this has been interpreted to mean that lateral partitioning into rafts at the TGN results in direct targeting of GPI-anchored proteins to apical membranes²⁰. However, this does not take into account the recent finding that GPI-anchored proteins undergo constitutive uptake from and recycling back to the plasma membrane^{16,17}. Such dynamic behaviour offers the alternative possibility of indirect trafficking to different plasma membrane domains, as observed in polarized hepatic cells^{18,24}.

Here, we investigate the pathway that GPI-anchored proteins follow *en route* to the apical domain of polarized MDCK cells. Employing a variety of methods for distinguishing between direct and indirect targeting pathways, we show that newly synthesized GPI-anchored proteins are first delivered to basolateral membranes adjacent to tight junctions and are then internalized by a non-clathrin pathway to the apical plasma membrane. This suggests the primary site for apical sorting of the GPI-anchored proteins is the lateral plasma membrane, rather than the TGN.

¹Cell Biology and Metabolism Branch, National Institute of Child Health and Human Development, National Institutes of Health, Bethesda, MD 20892, USA.

²Department of Cell Biology and Oncology, Istituto di Ricerche Farmacologiche “Mario Negri”, Consorzio Mario Negri Sud, 66030 Santa Maria Imbaro (Chieti), Italy.

³Correspondence should be addressed to J.L.S. (e-mail: jlippin@helix.nih.gov).

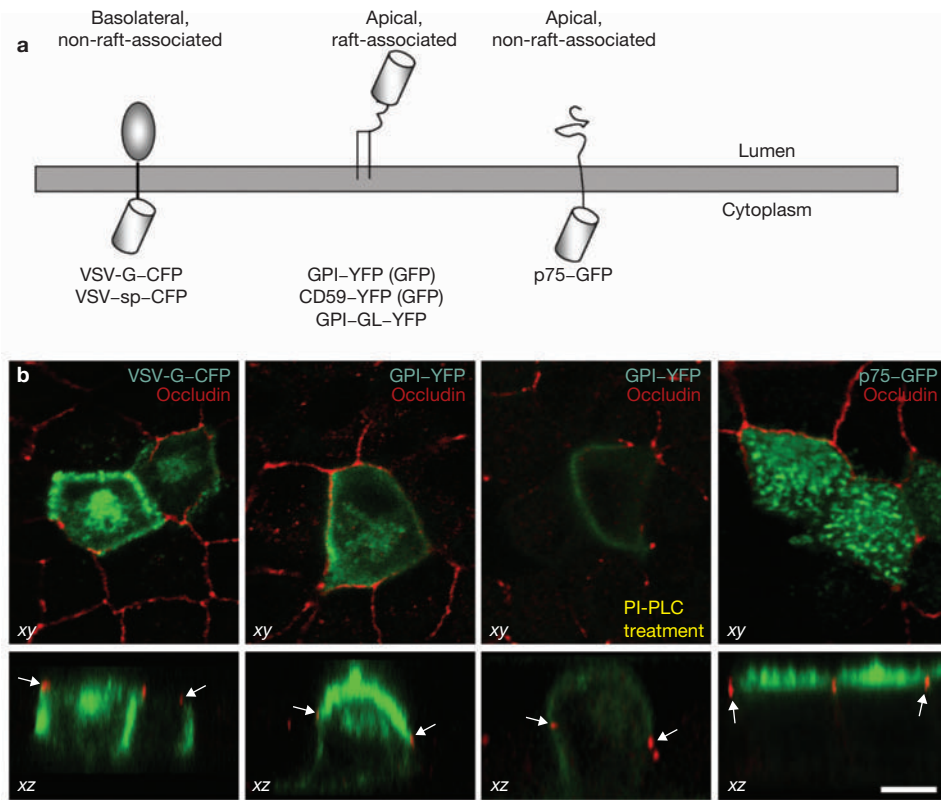


Figure 1 Apical and basolateral markers in polarized MDCK cells. (a) A schematic representation of fluorescent apical and basolateral markers used in this study. (b) MDCK cells grown on filters were transfected with VSV-G-CFP, GPI-YFP or p75-GFP and stained with an antibody against occludin. Confocal sections revealed that VSV-G-CFP is enriched at the

lateral surfaces of the cells, below tight junctions (arrows), whereas GPI-YFP and p75 are concentrated at the apical portion of the plasma membrane. PI-PLC treatment significantly decreased the amount of GPI-YFP at the apical surface. Scale bar represents 6.2 μm for all panels.

RESULTS

GFP-tagged apical and basolateral markers

As apical cargos, we used the raft-associated^{16,20} GPI-anchored proteins, GPI-YFP (yellow fluorescent protein), GPI-glycan-YFP (GPI-GL-YFP) and CD59-YFP¹⁶, or the non-raft protein, p75-GFP^{22,23} (Fig. 1a). As basolateral markers, we used the ts045-temperature sensitive mutant of vesicular stomatitis virus G protein, VSV-G, with²⁰ or without²⁵ a spacer sequence, and tagged with CFP (that is, VSV-G-CFP and VSV-G-sp-CFP; Fig. 1a). VSV-G-CFP (Fig. 1b) and VSV-G-sp-CFP (data not shown) were localized only on basolateral membranes in polarized MDCK cells, whereas GPI-YFP (Fig. 1b), GPI-GL-YFP (see Supplementary Information, Fig. S1), CD59-YFP (data not shown) and p75-GFP (Fig. 1b) were enriched on apical membranes. Addition of phosphatidylinositol-specific phospholipase C (PI-PLC; which digests GPI anchors) abolished the fluorescent signal of GPI-YFP (Fig. 1b), indicating that the chimera functioned as a GPI-anchored protein. The GFP-tagged markers are therefore sorted and targeted correctly in polarized cells.

Golgi-to-plasma-membrane trafficking of GPI-YFP and VSV-G-CFP in non-polarized cells

When VSV-G-CFP and GPI-YFP were co-expressed in non-polarized HeLa, COS-7 or MDCK cells, globular-tubular-shaped post-Golgi carriers (PGCs) containing both fusion proteins were observed budding from the TGN when cells were shifted from 20 °C (which causes proteins to accumulate in the TGN²⁶) to 32 °C (which allows protein

export from the TGN). This was observed in single images, where the two proteins often appeared in segregated domains within the same element (Fig. 2a, inset), or in time-lapse sequences (see Supplementary Information, Movie 1a–c). The yellow tracks, indicative of co-localized VSV-G-CFP and GPI-YFP fluorescence, were observed either in non-motile cells, which displayed curvilinear tracks (Fig. 2e, left), or in cells that had re-oriented towards a wound, which showed tracks preferentially directed toward the leading edge of the cell (Fig. 2e, right). Analysis of corresponding electron (Fig. 2b, c) and fluorescence (Fig. 2a) images by correlative light-electron microscopy²⁷ showed that an individual PGC containing GPI-YFP and VSV-G-CFP (see arrow and arrowhead in Fig. 2b, c) represented a single tubular carrier rather than a chain of small vesicles. VSV-G-CFP and GPI-YFP remained co-localized in PGCs until these structures fused with the plasma membrane, at which time fluorescence from both proteins quickly dispersed across the plasma membrane (Fig. 2f; also see Supplementary Information, Movies 1c and 2a, b).

To test whether other VSV-G constructs (VSV-G-sp-CFP) and GPI-linked proteins (GPI-GL-YFP and CD59-YFP) behaved similarly to or differently from VSV-G-CFP and GPI-YFP, we co-expressed them pair-wise in non-polarized cells and visualized their trafficking during warm-up from a 20 °C block. In all cases, a large fraction of the co-expressed proteins exited the TGN in common carriers (see Supplementary Information, Fig. S1). Taken together, the data suggest that in these non-polarized cells, VSV-G and GPI-anchored proteins travel in the same carriers from the Golgi to the plasma membrane.

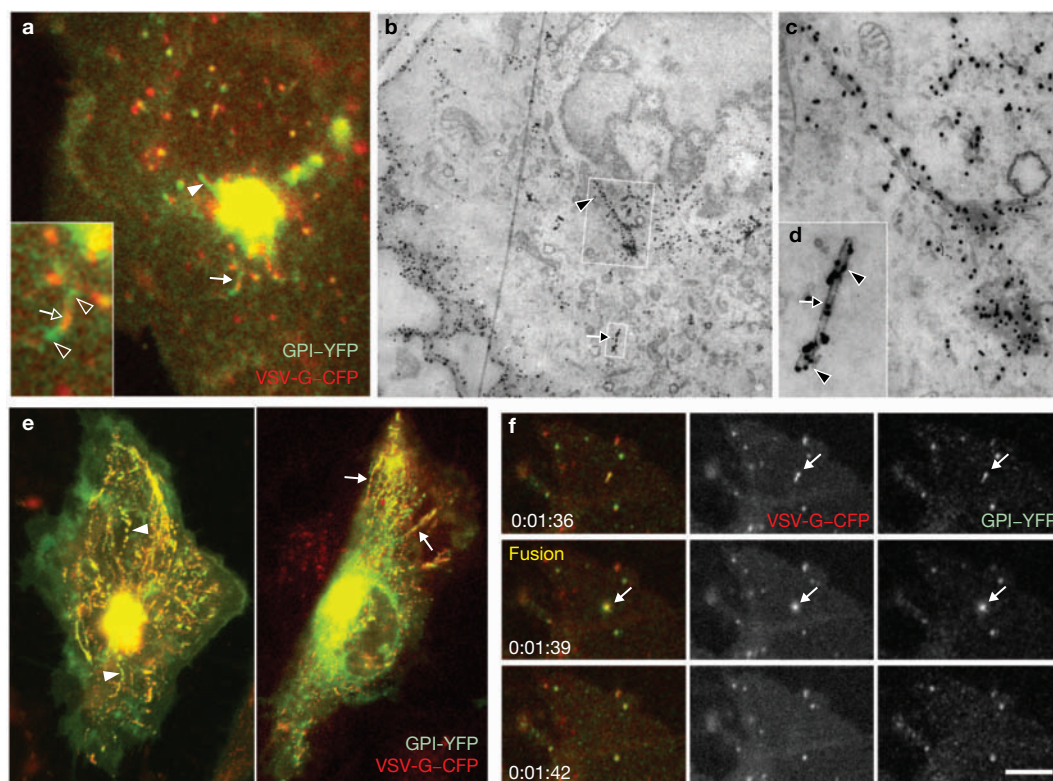


Figure 2 Exit of VSV-G and GPI from the Golgi complex. (a) Cells co-expressing VSV-G-CFP and GPI-YFP (which contains the Myc epitope) were incubated for 4 h at 40 °C, followed by 2 h at 20 °C to accumulate these markers in the TGN. Cells were then shifted to 32 °C and observed by confocal microscopy before fixation. The cell shown was fixed when one PGC was forming (arrowhead) and another had already detached from the Golgi (arrow), approximately 10 min after warm-up. An enlarged image of the detached PGC (inset) reveals that VSV-G-CFP (empty arrow) and GPI-YFP (empty arrowhead) are segregated into distinct domains. (b) The cell from **a** was immunogold labelled using an antibody to the Myc epitope in GPI-YFP, prepared and cut into serial sections. The same attached and free post-Golgi structures in **a**, indicated by the arrow and arrowhead, respectively, were identified (white boxes). (c) The enlarged image of the area within the large white box in **b** shows the complex tubular morphology of a PGC emerging from the Golgi. (d) An enlarged image of the area within the small box in **b**. Note the unequal distribution of gold labelling along the tubule, with more particles at the ends

(arrowheads) when compared with the middle of the tubule (arrow). (e) HeLa cells were transfected with VSV-G-CFP (red) and GPI-YFP (green), incubated for 4 h at 40 °C, followed by 2 h at 20 °C to accumulate both markers in the TGN. They were then observed at the confocal microscopy stage after shifting to 32 °C. Shown is a merged time-lapse sequence from a non-polarized cell (3-s intervals collected over 3 min, left; also see Supplementary Information, Movie 1a) and a cell migrating into a wound (3-s intervals collected over 1.5 min, right; also see Supplementary Information, Movie 1b). The presence of yellow tracks (see arrows and arrowheads) suggests that VSV-G-CFP and GPI-YFP move in common carriers. (f) Cells were treated and observed as in **e**. Time-lapse images from a small area at the periphery of a cell were collected. The data reveal the dispersal of the fluorescent signal for both VSV-G-CFP and GPI-YFP when the post-Golgi intermediates carrying these proteins fuse with the plasma membrane (see arrows). Time is indicated in hours, minutes and seconds. Scale bar represents 3.1 μm in **a**, 2.4 μm in **b**, 660 nm in **c**, 480 nm in **d**, 6.2 μm in **e**, and 3.5 μm in **f**.

Characteristics of VSV-G-CFP and GPI-YFP transport

As a previous study²⁰ reported that VSV-G-YFP and GPI-CFP sort into separate PGCs, further experiments were performed to clarify Golgi-to-plasma membrane transport of these proteins. In one experiment, we studied the effect of inhibiting detachment of transport intermediates from the TGN through expression of a kinase-dead mutant of protein kinase D (PKD^{K618N} (ref. 28); Fig. 3). Cells were transfected with VSV-G-CFP, GPI-YFP, and either wild-type or mutant PKD. They were then incubated at 20 °C to accumulate the proteins in the TGN before warming to 32 °C and analysis by dual-colour imaging. Normal packaging of VSV-G-CFP and GPI-YFP into PGCs and delivery to the plasma membrane were observed in cells expressing wild-type PKD (data not shown). However, these processes were inhibited in PKD^{K618N}-expressing cells, with the two markers found colocalized in elongated tubules still attached to the Golgi (Fig. 3a). This indicates that PKD activity is required for nascent transport intermediates containing VSV-G and GPI-anchored proteins to detach from the TGN.

Because VSV-G-CFP and GPI-YFP remained segregated as distinct, micron-sized domains within the nascent intermediates (Fig. 3b), lateral partitioning of VSV-G-CFP and GPI-YFP in the TGN occurs independently of PKD.

In a different experiment, we investigated whether VSV-G-CFP and GPI-YFP remain localized in PGCs when fusion with the plasma membrane is inhibited by microinjection of mutant αSNAP protein²⁹, whose expression inhibits fusion at the plasma membrane³⁰. Non-polarized cells co-expressing VSV-G-CFP and GPI-YFP at 20 °C were microinjected with the αSNAP mutant and then shifted to 32 °C. Only in microinjected cells was delivery to the plasma membrane inhibited, with VSV-G-CFP and GPI-YFP co-localizing in numerous small carriers at the cell periphery (Fig. 4a, left-hand cell). Quantification revealed that virtually every carrier contained significant amounts of both VSV-G-CFP and GPI-YFP (Fig. 4b).

Membrane fusion was also blocked with tannic acid, a cell-impermeable fixative³¹ used previously to prevent secretory granule exocytosis

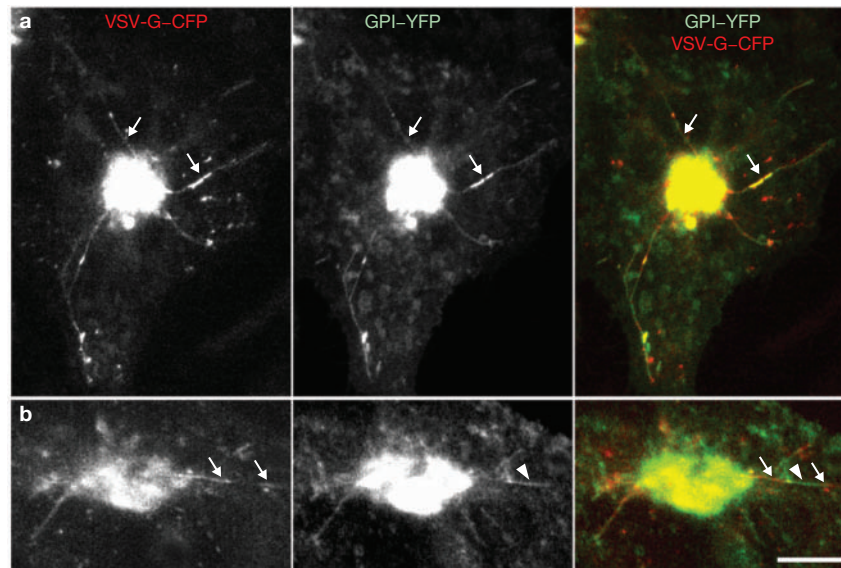


Figure 3 VSV-G-CFP and GPI-YFP localize within the same PGC precursors. HeLa cells expressing PKD^{K618N} were transfected with VSV-G-CFP and GPI-YFP, incubated at 40 °C for 4 h and then at 20 °C for 2 h to accumulate both markers in the TGN. Cells were then warmed to 32 °C and observed by confocal microscopy. Two examples of expressing

cells are shown (**a** and **b**). Arrows point to tubule elements still attached to the TGN as a result of expressing the PKD mutant. These elements contain both VSV-G-CFP and GPI-YFP, with the two markers showing areas of lateral segregation (**b**, arrows and arrowhead). Scale bar represents 3.5 μm.

and endocytosis³¹. Tannic acid blocked plasma membrane fusion of PGCs containing VSV-G-CFP (Fig. 4d, e; also see Supplementary Information, Movie 3a), with no effect on ER-to-Golgi trafficking of VSV-G-CFP (see Supplementary Information, Movie 3b) or on short-term cell viability. To analyse the effect of tannic acid on VSV-G-CFP and GPI-YFP distribution, non-polarized MDCK cells co-expressing these proteins were incubated at 20 °C to accumulate the proteins in the TGN and then shifted to 32 °C for 1 h in the presence or absence of tannic acid. In untreated cells, both proteins were efficiently delivered to the plasma membrane (Fig. 4c), whereas in tannic-acid-treated cells the proteins co-localized in PGCs that had accumulated at the cell periphery (Fig. 4d). Quantification demonstrated that in tannic-acid-treated cells, virtually all GPI-YFP-containing PGCs also contained VSV-G-CFP fluorescence, and *vice versa* (Fig. 4f). Similar results were observed in MDCK cells expressing either CD59-YFP and VSV-G-CFP (Fig. 4e, g), or GPI-GL-YFP and VSV-G-sp-CFP (data not shown). Thus, VSV-G-CFP and GPI-anchored proteins remain co-localized in PGCs when fusion with the plasma membrane is inhibited.

Use of tannic acid to dissect VSV-G-CFP and GPI-YFP trafficking in polarized cells

Because tannic acid inhibits plasma membrane fusion within seconds of treatment and does not pass through tight junctions (see below), it can be added selectively to different polarized domains, making it suitable as a tool for preferentially inhibiting fusion of membrane-bound carriers at either apical or basolateral domains. Therefore, we used tannic acid to investigate the trafficking itinerary of VSV-G-CFP and GPI-YFP in polarized MDCK cells.

We focused first on the effect of tannic acid on VSV-G-CFP trafficking. In untreated cells, VSV-G-CFP molecules were delivered efficiently from the Golgi (Fig. 5a) to the lateral plasma membrane (Fig. 5b) within 45 min of warm-up from a 20-°C block. However, when tannic acid was added to the basolateral medium to inhibit basolateral exocytosis, no plasma membrane delivery of VSV-G-CFP occurred (Fig. 5c).

Instead, PGCs enriched in VSV-G-CFP were observed near the ring of tight junctions surrounding the cell. In contrast, when tannic acid was added to the apical medium, VSV-G-CFP was readily delivered to lateral membranes and no PGCs containing VSV-G-CFP accumulated (Fig. 5d).

We next examined the effect of tannic acid on trafficking of GPI-YFP (Fig. 5e-h). In untreated cells, the Golgi-localized GPI-YFP pool (Fig. 5e) readily redistributed to the apical plasma membrane after warm-up from a 20 °C block (Fig. 5f). However, when tannic acid was added to the basolateral medium to inhibit basolateral exocytosis (Fig. 5g), apical delivery of GPI-YFP was completely inhibited, with GPI-YFP retained in numerous small transport intermediates located in the plane adjacent to tight junctions. When tannic acid was added selectively to the apical surface (Fig. 5h), GPI-YFP molecules also failed to be delivered to apical membranes at 32 °C, but the transport intermediates that accumulated were larger than those observed after addition of tannic acid to the basolateral medium, and they were more abundant in *xy* planes above tight junctions.

To determine if the polarized transport of VSV-G-CFP and GPI-YFP intersect at any step, the effect of tannic acid in cells co-expressing these proteins was examined (Fig. 6a-g). Addition of tannic acid to the basolateral medium led to both proteins accumulating in the same carriers adjacent to tight junctions when cells were shifted from 20 °C to 32 °C for either 45 min or 90 min (Fig. 6c, f). When tannic acid was added to the apical medium, however, VSV-G-CFP redistributed throughout basolateral membranes, whereas GPI-YFP accumulated in carriers above the zone of tight junctions (Fig. 6d, g).

These results suggested that after export from the TGN, GPI-anchored proteins and VSV-G-CFP are transported in common carriers to a zone of lateral membrane adjacent to tight junctions. After fusion of the carrier with plasma membrane at this site, VSV-G-CFP and GPI-anchored proteins undergo rapid segregation, with VSV-G-CFP redistributing throughout basolateral membranes and GPI-anchored proteins internalizing into apically directed transport intermediates.

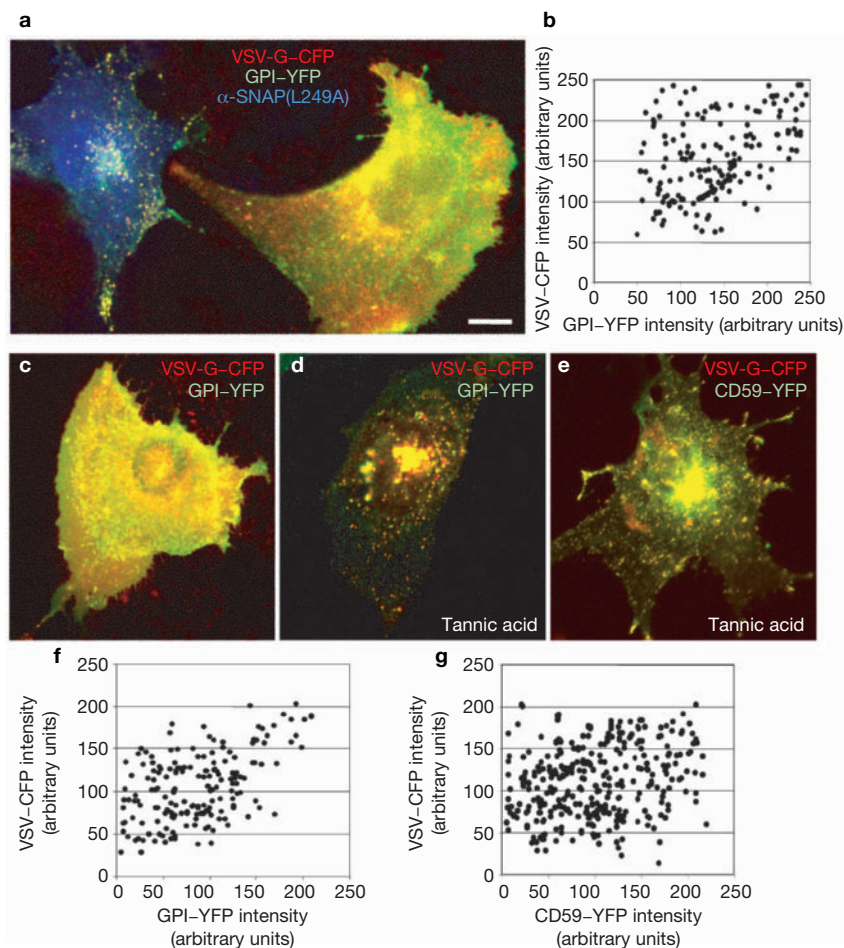


Figure 4 Tannic acid treatment identifies VSV-G-CFP and GPI-YFP in the same post-Golgi carriers. **(a)** Non-polarized MDCK cells expressing VSV-G-CFP and GPI-YFP were microinjected with the L249A α -SNAP mutant (mixed with TRITC-dextran) during incubation at 20 °C to accumulate the proteins in the TGN. Cells were then shifted to 32 °C for 45 min, fixed and observed by confocal microscopy. The microinjected cell (left) accumulated PGCs containing both VSV-G-CFP and GPI-YFP, whereas in the non-injected cell (right), both proteins were efficiently delivered to plasma membrane. **(b)** Intensities of VSV-G-CFP and GPI-YFP fluorescence were quantified within individual PGCs in MDCK cells

injected with L249A α -SNAP, as in **a**. **(c, d)** MDCK cells transfected with VSV-G-CFP and GPI-YFP were incubated at 40 °C for 4 h and then at 20 °C for 2 h to accumulate both proteins in the TGN. Cells were then warmed to 32 °C for 45 min in the presence **(c)** or absence **(d)** of 0.5% tannic acid, fixed and observed under the confocal microscope. **(e)** MDCK cells expressing VSV-G-CFP and CD59-YFP were treated as in **d** and observed by confocal microscopy. **(f, g)** Fluorescence intensities of VSV-G-CFP and GPI-YFP **(f)** or VSV-G-CFP and CD59-YFP **(g)** were quantified within individual post-Golgi carriers, as described as in **d** and **e**, respectively. Scale bar represents 7.2 μ m in **a, c–e**.

To determine whether non-raft-associated, apical proteins targeted similarly to or differently from GPI-YFP, we investigated the behaviour of p75-GFP after release from a 20-°C block in polarized MDCK cells (Fig. 5i–l). Delivery of p75-GFP to apical domains was inhibited when tannic acid was added to the apical medium. However, in contrast to GPI-anchored proteins, apical delivery of p75-GFP still occurred when tannic acid was added to the basolateral medium. This suggests that p75 follows a direct route from the TGN to apical membranes in polarized cells.

Characterization of GPI-YFP transcytosis

To characterize GPI-YFP transcytosis, we added horseradish peroxidase (HRP) as transcytotic tracer to the basolateral medium of polarized MDCK cells expressing GPI-YFP at 20 °C (Fig. 7a–c). After 45 min of warm-up to 32 °C, many GPI-YFP-containing carriers contained HRP (Fig. 7a). Evidence that such co-localization resulted from GPI-YFP

being delivered to the basolateral plasma membrane and then being internalized with HRP was obtained from experiments in which tannic acid was added to the basolateral medium, causing membrane traffic at basolateral membranes to be blocked. After shifting from 20 °C to 32 °C under these conditions, no uptake of HRP into cells was observed and GPI-YFP resided in carriers that did not contain any HRP (Fig. 7b). When tannic acid was instead added to the apical medium, HRP and GPI-YFP co-localized in many intracellular structures (Fig. 7c).

Further support for transcytosis of GPI-YFP was obtained by adding a Cy3-conjugated anti-Myc antibody (which recognizes the Myc tag within GPI-YFP) to the basolateral medium of cells expressing GPI-YFP. After 15 min on ice, cells were washed and placed in fresh medium at 37 °C. Immediate imaging of cells revealed anti-Myc antibody staining only at basolateral membranes, where only small amounts of GPI-YFP were located (Fig. 8a, b). After incubation of the cells for 2 h at 37 °C, however, the antibody label was now redistributed

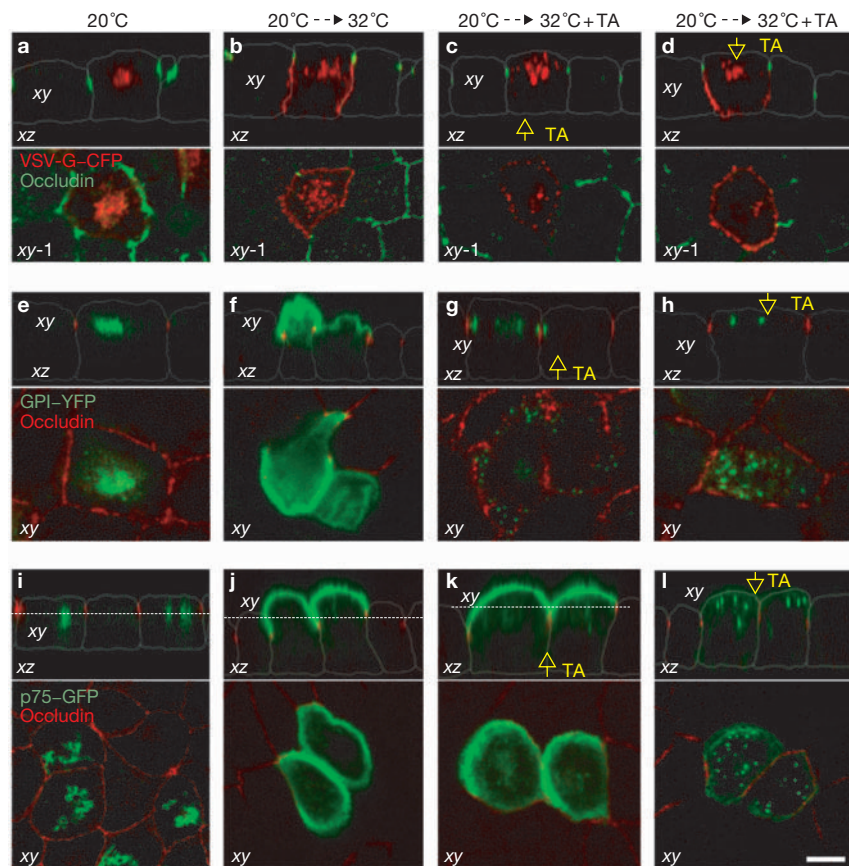


Figure 5 Spatial organization of apical and basolateral marker transport in polarized MDCK cells. **(a–d)** MDCK cells grown on filters were transfected with VSV-G-CFP and incubated for 4 h at 40 °C and then for 4 h at 20 °C to accumulate the protein in the TGN **(a)**. Cells were then warmed to 32 °C under three different conditions: in the absence of tannic acid **(b)**, or with tannic acid (TA) added basolaterally **(c)** or apically **(d)**. After 45 min at 32 °C, the cells were fixed, stained with anti-occludin antibodies and optically sectioned by confocal microscopy. The top panels show xz sections of these cells. The lower panels are xy images of lines (xy) shown in the top panel. **(e–h)** MDCK cells grown on filters were transfected with GPI-YFP. The apical medium was treated with PI-PLC to remove apical GPI-YFP and cells were shifted to 20 °C for 4 h to accumulate the newly-synthesized protein in the Golgi **(e)**. The cells were warmed to 32 °C in the absence of tannic acid **(f)**,

or with tannic acid added basolaterally **(g)** or apically **(h)**. After 45 min at 32 °C, cells were then fixed, stained with anti-occludin antibodies and optically sectioned by confocal microscopy. The top panels show xz sections of these cells. The bottom panel shows an xy image of the line (xy) shown in the top panel. **(i–l)** MDCK cells grown on filters were transfected with p75-GFP, and after 2 h at 37 °C were shifted to 20 °C for 4 h to accumulate the protein in the Golgi **(i)**. The cells were then warmed to 32 °C under three different conditions: without tannic acid **(j)**, with tannic acid added basolaterally **(k)** or with tannic acid added apically **(l)**. After 45 min at 32 °C, the cells were then fixed, stained with anti-occludin antibodies and optically sectioned by confocal microscopy. The top panels show xz sections of these cells. The bottom panel shows an xy image of the line (xy) shown in the top panel. Scale bar represents 6 μ m in all panels.

to the apical plasma membrane, where GPI-YFP was abundant (Fig. 8c, d).

Transcytosis of GPI-YFP was also demonstrated by a biochemical approach (Fig. 8e, f). PI-PLC was added to the basolateral medium to remove GPI-YFP from basolateral membranes. After incubating for various times, the cells were washed and PI-PLC was added to the apical medium to harvest GPI-YFP at the apical surface. If the pool of GPI-YFP at the apical surface derives primarily from basolateral membranes, then this protocol should cause a reduction in apical GPI-YFP levels over time. Consistent with this prediction, western blot analysis of GPI-YFP (Fig. 8e) revealed that after 2 h, only 30% of GPI-YFP was detected at the apical plasma membrane relative to control cells (Fig. 8f).

GPI-linked proteins are internalized at lateral membranes in non-clathrin structures

The morphology of the transcytotic intermediates carrying GPI-YFP

to apical surfaces was examined by electron microscopy in GPI-YFP-expressing cells in which HRP was added to the basolateral medium during temperature shift from 20 °C to 32 °C (Fig. 7d). In addition to being found in HRP-positive endocytic structures, GPI-YFP was frequently found concentrated in grape-like profiles (characteristic of caveolae) attached to the plasma membrane (Fig. 7d, arrowhead). GPI-YFP labelling was never found in association with clathrin-coated buds (Fig. 7d, arrow). Therefore, these results suggest that uptake of GPI-YFP at lateral domains of MDCK cells occurs in a clathrin-independent fashion.

DISCUSSION

GPI-anchored proteins have traditionally been thought follow a direct pathway from the Golgi to the apical plasma membrane of polarized MDCK cells. This model is based on the low abundance of these proteins on the basolateral plasma membrane and their failure to accumulate at

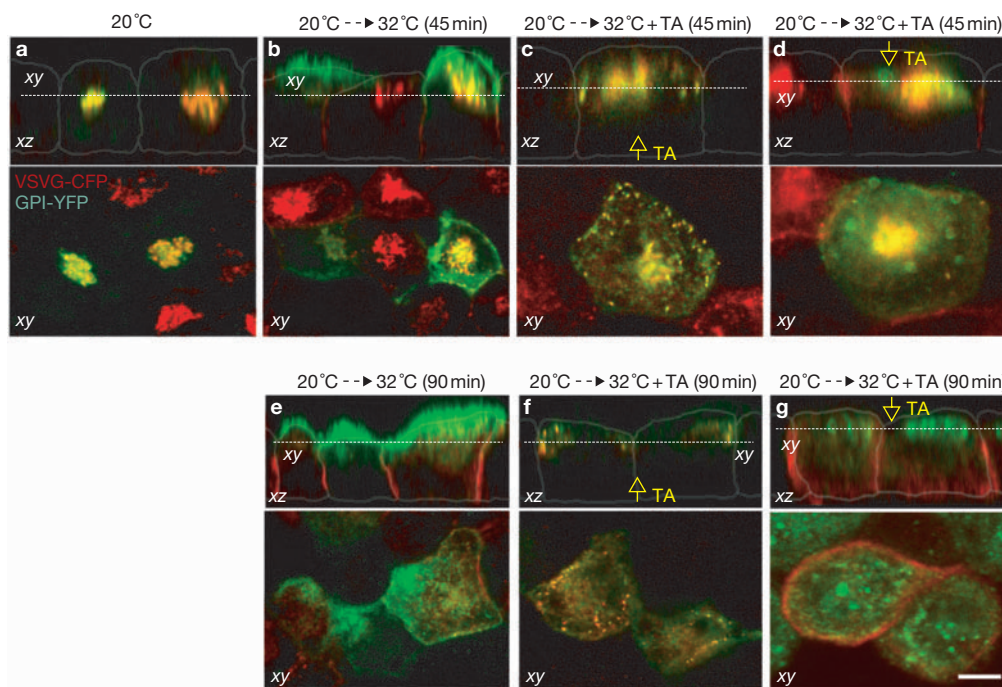


Figure 6 VSV-G-CFP and GPI-YFP are delivered to the basolateral plasma membrane in the same carriers. Filter-grown MDCK cells were co-transfected with GPI-YFP and VSV-G-CFP. The cells were then incubated at 40 °C for 4 h, followed by 20 °C for 4 h to accumulate the proteins in the TGN. When the cells were at 20 °C, they were treated with PI-PLC to remove all GPI-YFP from the plasma membrane (a). The cells were then shifted to

32 °C under three different conditions: no tannic acid treatment (b, e), with tannic acid added basolaterally (c, f), or with tannic acid added apically (d, g). After 45 min (b–d) or 90 min (e–g) of incubation at 32 °C, the cells were fixed and prepared for confocal microscopy. The top panels show xz sections of these cells. The bottom panel shows an xy image of the line shown in the top panel (xy). Scale bar represents 5.8 μm in a–g.

basolateral surfaces before appearing apically in biochemical pulse–chase labelling experiments^{32,33}. Relying on the localization of cholesterol-enriched lipid rafts at both the TGN and apical plasma membrane³⁴ and the affinity of GPI-anchored proteins for rafts^{34–36}, the model proposes that the GPI-linked proteins segregate into raft-enriched carriers in the TGN and are then directed separately to the apical plasma membrane^{3,20}.

The data in this study support an alternative model. Using live-cell imaging and selective inhibition of apical and basolateral exocytosis, we found that GPI-anchored proteins (including GPI-YFP, CD59-GFP and GPI-GL-YFP) are packaged together with basolateral cargo into TGN-derived carriers that travel to basolateral, rather than apical, membranes. The carriers are targeted to an area of lateral plasma membrane adjacent to tight junctions that are enriched in the exocyst complex. After fusing with these membranes, the GPI-anchored proteins are rapidly internalized into transcytotic carriers that are delivered to apical membranes, while basolateral proteins remain behind. These findings support a model in which GPI-anchored proteins in polarized MDCK cells follow an indirect pathway to the apical plasma membrane (Fig. 8g). An appealing feature of this model is that it provides a way for cells to utilize GPI-anchored proteins delivered to their plasma membrane for multiple purposes, rather than as an end state.

Indirect targeting of GPI-anchored proteins to the apical plasma membrane of polarized MDCK cells is consistent with recent findings in non-polarized cells, showing that GPI-anchored proteins at the plasma membrane are continuously taken up by a non-clathrin-dependent pathway and recycled back to the plasma membrane^{16,17}. It also fits with recent data showing that GPI-GFP proteins in polarized

hepatic cells follow an indirect pathway to apical membranes¹⁸. This raises the possibility that apical sorting of these GPI-anchored proteins in both kidney and liver cells occurs through a similar mechanism. The failure of biochemical studies in polarized MDCK cells to identify an indirect pathway for delivery of GPI-anchored proteins to apical membranes^{32,33} can be explained by the short period of time these proteins spend at the basolateral plasma membrane before being endocytosed and delivered to the apical plasma membrane.

The indirect targeting model provides the first explanation for why caveolae in polarized MDCK cells are found only on the basolateral, and not the apical, plasma membrane³⁷. Caveolae are raft-enriched plasma membrane invaginations that are thought to be involved in the internalization of lipid rafts and their associated cargo^{38,39}. In the indirect trafficking model, caveolae could help take up raft-associated, GPI-anchored, proteins at the basolateral surface into a transcytotic pathway distinct from the clathrin-mediated, transcytotic, pathway followed by polymeric IgR^{40, 41}. This explanation is consistent with our finding that soon after release from the TGN, the GPI-anchored proteins are located in caveolae-like structures at the basolateral plasma membrane. It also helps explain why in cells lacking caveolae (for example, FRT cells), GPI-anchored proteins mis-localize to basolateral domains⁴², as this is what would be expected if caveolae are necessary but not sufficient⁴³ for transcytosis of the GPI-anchored proteins.

Evidence for the rapid basolateral routing of GPI-anchored proteins came from our use of a novel method — tannic acid treatment — to selectively inhibit basolateral and/or apical fusion events. When basolateral exocytosis was inhibited through addition of tannic acid to the basolateral medium, GPI-YFP molecules exported from the TGN were

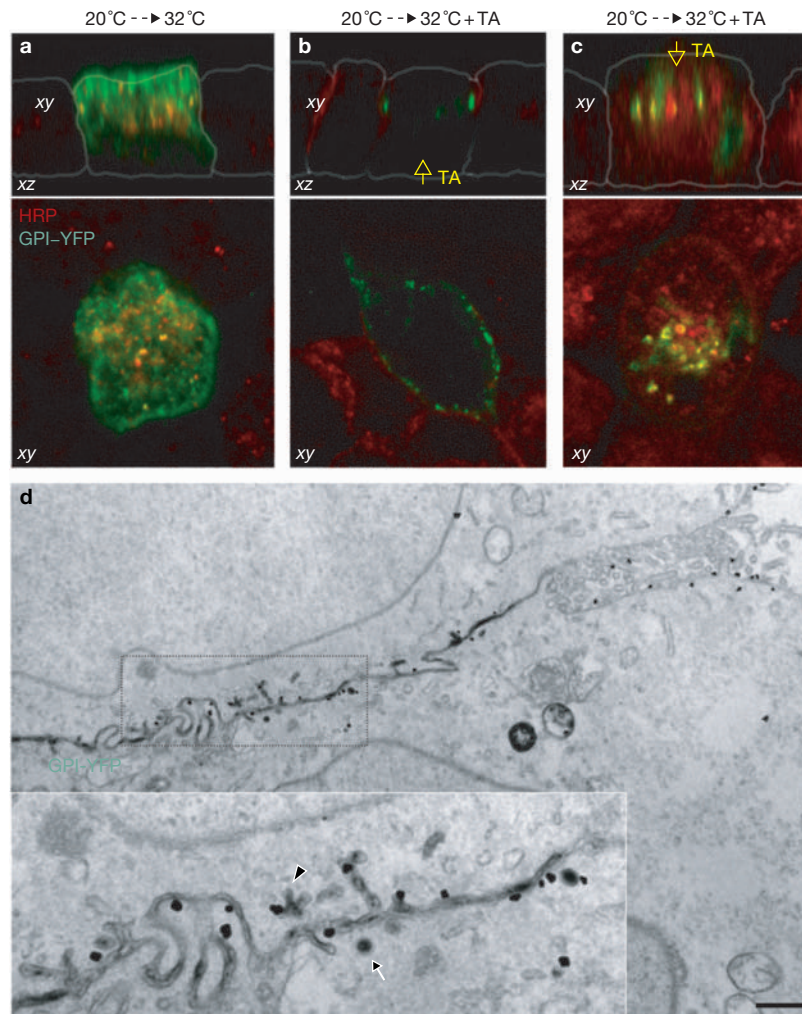


Figure 7 Distribution of GPI-YFP within transcytotic carriers (**a–c**) Filter-grown, polarized MDCK cells expressing GPI-YFP were incubated at 20 °C for 4 h to accumulate the chimaera in the TGN. The cells were warmed to 32 °C with HRP added to the basolateral medium under three conditions: no tannic acid treatment (**a**), or with tannic acid added basolaterally (**b**) or apically (**c**). After 45 min of incubation at 32 °C, the cells were fixed, stained with anti-HRP antibody and optically sectioned by confocal microscopy. (**d**) Filter-grown, polarized MDCK cells expressing GPI-YFP were incubated at 20 °C for 4 h to accumulate the chimaera in the TGN. The cells were warmed to 32 °C with HRP added to

the basolateral medium. After 45 min of incubation at 32 °C, the cells were fixed, immunogold-labelled with an anti-GFP antibody and prepared for electron microscopy. The basolateral surface with highest gold labelling is shown in the boxed area, which was near the tight junctional zone. An enlargement of the boxed area shows a variety of HRP-labelled endocytic structures, including a clathrin-coated vesicle (arrow) and a caveolae-like, non-coated structure (arrowhead). HRP and gold particles (indicative of GPI-YFP labelling) were co-distributed only in the non-coated endocytic structures. Scale bar represents 5.5 μm in **a–c**, 580 nm in **d**, an 200 nm in the inset of **d**.

unable to reach the apical plasma membrane. Instead, they were found in carriers containing VSV-G-CFP in close proximity to the lateral plasma membrane adjacent to tight junctions. Importantly, this treatment had no effect on apical delivery of p75-GFP, which has been reported to follow a direct pathway to apical membranes²². When tannic acid was added selectively to the apical medium, VSV-G-CFP molecules derived from the TGN were readily delivered to the basolateral surface, but apical delivery of GPI-YFP molecules was inhibited. The carriers containing GPI-YFP under these conditions were different from those observed when tannic acid was applied basolaterally — they did not contain VSV-G-CFP and they could be labelled with basolaterally derived endocytic tracer.

The indirect pathway supported by these experiments exhibited several properties relevant for understanding the localization of sorting

and trafficking machinery in polarized cells. First, GPI-YFP and VSV-G-CFP proteins were not sorted into separate carriers before delivery to the basolateral plasma membrane, but were found in the same post-Golgi carriers when basolateral exocytosis was inhibited with tannic acid. This suggests that the apical and basolateral sorting signals on these proteins operate after the proteins have been delivered to the basolateral membrane. A post-plasma-membrane sorting mechanism is also consistent with other studies¹³ showing that low-density lipoprotein receptors (LDLRs) are transported directly from the TGN to the basolateral surface in cells lacking AP-1B (the adaptor responsible for basolateral targeting/retention of LDLRs¹²).

Second, TGN-derived carriers enriched in GPI-YFP and VSV-G-CFP did not appear to fuse with the entire basolateral surface, but only with sites restricted to a region of lateral plasma membrane adjacent to tight

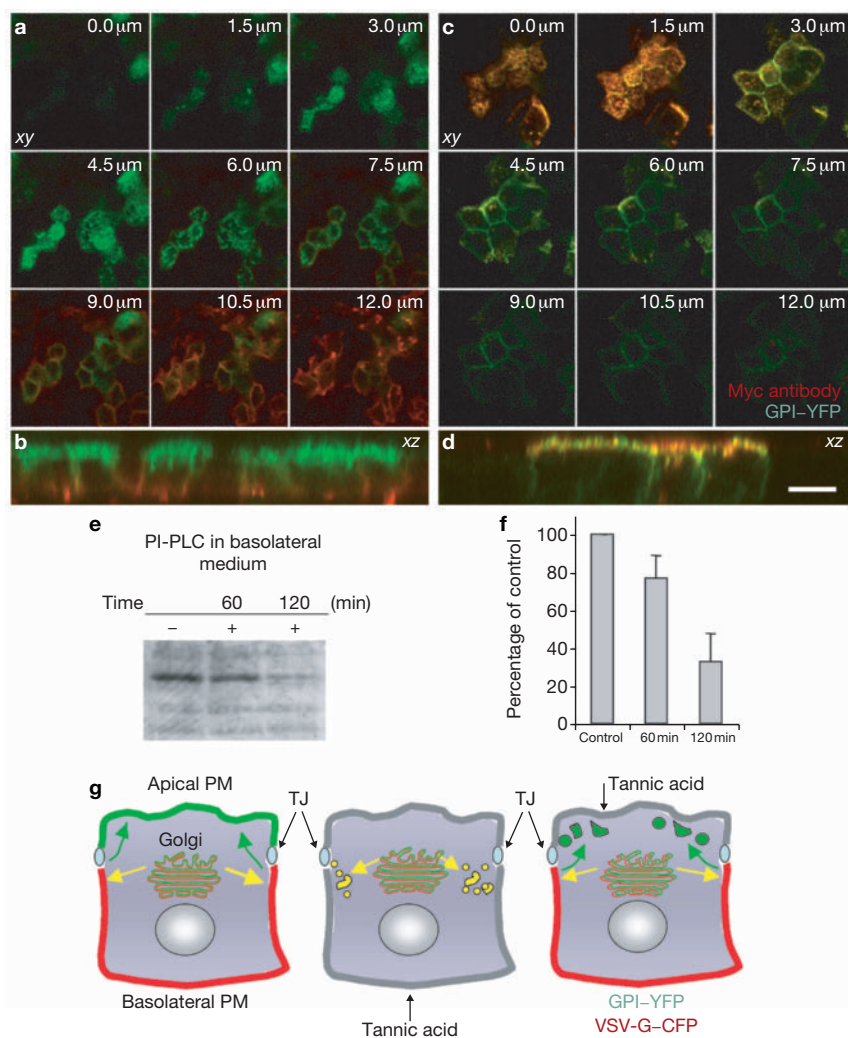


Figure 8 Transcytosis of GPI-GFP in polarized MDCK cells. **(a–d)** Filter-grown MDCK cells were transfected with GPI-YFP and incubated at 4 °C for 15 min with Cy3 conjugated anti-Myc antibody added to the basolateral medium. Some filters were fixed immediately **(a, b)** and others were washed and shifted to 37 °C for 2 h **(c, d)** and only then fixed and prepared for confocal microscopy. *xy* and *xz* images reveal that at 4 °C, antibody binds to the Myc tag of GPI-GFP only at the basolateral surface of the cells **(a, b)** while after 2 h at 37 °C, the antibody was transported to the apical surface of the cells **(c, d)**. **(e, f)** PI-PLC was added for 1 or 2 h to the basolateral surface of filter-grown MDCK cells stably expressing

GPI-GFP. After incubation, control and treated cells were washed and GPI-GFP was harvested from the apical surface into apical medium by PI-PLC treatment. The medium specimens were then analysed by SDS-PAGE. Quantification **(f)** of bands in the western blot **(e)** stained with the anti-GFP antibody showed a significant decrease of GPI-GFP signal at the apical surface after a 2-h PI-PLC treatment of the basolateral surface of the cells. **(g)** A model illustrating GPI-YFP and VSV-G-CFP trafficking in polarized MDCK cells and the effects of tannic acid (see Discussion). PM, plasma membrane; TJ, tight junction. Scale bar represents 28 μm in **a** and **b**, and 12 μm in **c** and **d**.

junctions. This confirms the result of an earlier study, reporting apical markers near sites of cell–cell contact⁴⁴, and also supports recent work in which monitoring of fusion events along basolateral membranes with total internal reflection microscopy showed that fusion activity occurred laterally and far from basal surfaces²². Because the plasma membrane sites at which GPI-YFP- and VSV-G-CFP-containing PGCs fused are enriched in the exocyst — an evolutionarily conserved protein complex responsible for exocytosis of constitutive secretory carriers^{22,45} — polarized cells have developed a system for organizing exocyst components at these specialized cell-surface domains and for directing TGN-derived carriers to this region.

Third, our data indicate that partitioning into rafts at the TGN is not the major determinant for apical delivery by a direct, TGN-to-apical-plasma-membrane, pathway. Consistent with this, recent studies have

shown that removal of the GPI-anchor from several apical GPI-anchored proteins does not prevent them from being targeted by a direct pathway to apical membranes^{46,47}, whereas removal of their glycosylation signal(s) results in mis-targeting of the apical proteins to basolateral membranes^{46–48}. Thus, it seems that alternative signals (for example, *N*- and *O*-glycosylation) to those that result in partitioning of a protein into rafts (that is, a GPI-anchor) are necessary for directing a protein into the direct pathway from the TGN to the apical plasma membrane^{6,7,46–48}.

Finally, our finding that export of GPI-anchored proteins from the TGN is dependent on PKD extends other studies²⁸, by showing that, in addition to basolateral cargo, raft-associated proteins trafficking indirectly to apical domains depend on this kinase for TGN export. The mechanism of such export needs further exploration, but seems to

involve protein sorting into micron-sized domains of the TGN that are depleted of Golgi enzymes^{19,20,49}. □

METHODS

Cell culture. MDCK, COS-7, HeLa and BHK cells were cultured in DMEM (Gibco, Invitrogen SRL, Milan, Italy) supplemented with 10% foetal calf serum (FCS) and 1 mM L-glutamine. HeLa cells expressing PKD^{K618N} were obtained from V. Malhotra (La Jolla, CA) and cultured in the same medium containing G418. Confluent HeLa cell monolayers were locally wounded, and 4 h later cells migrating into the wound were examined.

Antibodies, DNA and other reagents. The cDNAs of YFP-GL-GPI and VSV-G3-SP-CFP were kindly provided by K. Simons (Dresden, Germany); the cDNA of the L294A α -SNAP mutant was from V.R.D. Burgoyne (Liverpool, UK); the cDNAs of GST-tagged wild-type and mutant PKD were from V. Malhotra; the cDNA of p75-GFP was from E. Rodriguez-Boulan (New York, NY); monoclonal antibodies against VSV-G, Myc tag, secondary IgG-Cy3 conjugates, PI-PLC and HRP were from Sigma-Aldrich (Milan, Italy); the polyclonal antibody against GFP was from Abcam (Cambridge, UK); monoclonal and polyclonal antibodies against occludin were from BD Biosciences (San Jose, USA). The Alexa-488, -546, -633-IgG conjugates, and TRITC and FITC dextrans were from Molecular Probes (Leiden, The Netherlands). The Nanogold gold-antibody conjugates and the Goldenhance electron microscopy kit were from Nanoprobes (Stony Brook, NY).

Cell transfection and infection with VSV. Fugene 6 reagent (Roche, IN) or Lipofectamine 2000 (Invitrogen, CA) were used for cDNA transfections of sub-confluent cells. Lipofectamine 2000 was used for transfection of tight MDCK monolayers grown on filters. To produce a cell line stably expressing GPI-YFP, transfected MDCK cells were grown in DMEM containing 800 $\mu\text{g ml}^{-1}$ G418.

The infection of sub-confluent cells stably expressing GPI-GFP with VSV was performed as described²⁷. The infection of MDCK monolayers grown on filters was performed as previously described⁵⁰. Briefly, monolayers of MDCK cells stably expressing GPI-GFP were infected with VSV in the presence of DEAE-dextran, washed and incubated at 40 °C for 4–5 h, and then incubated at 20 °C in the presence of 0.5 $\mu\text{g ml}^{-1}$ PI-PLC to synchronize VSV-G and GPI-GFP in the Golgi. Next, cells were washed and shifted to 32 °C to monitor exit of both proteins from the Golgi.

Microinjection. MDCK cells transfected with VSV-G-CFP and GPI-YFP were maintained at 40 °C overnight, and then at 20 °C for 1.5 h. Cells were then microinjected with 3.5 mg ml^{-1} of the L294A α -SNAP mutant mixed with TRITC-dextran using an Eppendorf transjector 5246 (Eppendorf, Milan, Italy) at 20 °C, and further incubated at 20 °C for 30–40 min to ensure binding of the mutant protein. Cells were then shifted to 32 °C for different times (up to 1 h) to release both proteins from the Golgi and then fixed.

Tannic acid treatment. Sub-confluent MDCK, HeLa and COS-7 cells were transfected with VSV-G-CFP and GPI-YFP. After 4 h at 37 °C, to allow the DNA to be taken up, cells were incubated for 4 h at 40 °C to accumulate VSV-G-CFP in the endoplasmic reticulum, and then for 2 h at 20 °C to accumulate both VSV-G-CFP and GPI-YFP in the TGN. The GPI-YFP pool at the plasma membrane was removed by treatment with 0.5 $\mu\text{g ml}^{-1}$ PI-PLC for 30 min during the course of the 20 °C block, or was selectively bleached at the confocal microscopy stage. In some cases, cells were observed under the confocal microscope *in vivo* at 32 °C. Alternatively, 0.5% tannic acid (Sigma-Aldrich) was added to the medium 10 min before release from the 20 °C block. Next, tannic-acid-treated cells and control cells were fixed for confocal microscopy 15 or 45 min after temperature shift to 32 °C. Polarized MDCK cells were grown on Transwell filters inserts (Corning, NY) for 2–3 days to obtain electrically tight monolayers (>100 $\Omega \text{ cm}^{-2}$) and then were cotransfected with VSV-G-CFP and GPI-YFP or transfected with GPI-GFP alone and infected with VSV. Cells were incubated at 40 °C for 4–5 h to accumulate VSV-G-FP (or VSV-G) within the endoplasmic reticulum. Cells were then incubated at 20 °C to accumulate newly synthesized VSV-G and GPI-FP within the Golgi. GPI-FP was removed from the surface of the cells by PI-PLC treatment during the course of the 20 °C block. At 10 min before the temperature shift from 20 °C to 32 °C, tannic acid was added to

either the apical or basolateral medium of Transwell filters inserts, and tannic acid-treated and control cells were fixed 30, 60 or 120 min later and examined by confocal microscopy.

Similar experiments were performed with filter-grown MDCK cells transfected with only one of the fusion proteins: CD59-FP, VSV-G-FP, GPI-FP or p75-FP. At the end of the 20 °C block release and tannic acid treatment, these cells were fixed and stained with an anti-occludin antibody to observe the border between the apical and basolateral surface. In the other set of experiments, fully polarized MDCK cells were transfected with GPI-FP and the next day were treated with PI-PLC immediately during incubation at 20 °C for 3 h. Tannic acid was added to either the apical or basolateral medium 10 min before shifting the temperature from 20 °C to 32 °C. Simultaneously with this warm-up, HRP (5 mg ml^{-1}) was added to the basolateral chamber of the filters inserts and cells were incubated for 30, 60 or 120 min at 32 °C, fixed, and then stained with an anti-HRP antibody.

Transcytosis assays. Filter-grown MDCK cells transfected with GPI-GFP were incubated at 4 °C for 15 min with Cy3-conjugated anti-Myc Ab added to the basolateral medium. Some filters were fixed immediately after 4 °C incubation, whereas others were washed and shifted to 37 °C for 2 h and only then fixed and prepared for confocal microscopy to evaluate colocalization of endocytosed antibody with GFP. Biochemical evaluation of transcytosis was based on the idea that removal of protein from the basolateral surface will result in a decrease of its amount at the apical domain of the plasma membrane⁴¹. Therefore, to remove GPI-GFP from the basolateral surface, tight monolayers of MDCK cells stably expressing GPI-GFP were incubated with PI-PLC added to the basolateral medium for 1 and 2 h. To detect GPI-GFP signal at the apical surface, cells were washed and PI-PLC was added to the apical medium (30 min on ice) to harvest GPI-FP from the apical domain of the plasma membrane. Next, specimens of apical medium from control and treated cells containing cleaved GPI-FP were subjected to SDS-PAGE and western blotting with an anti-GFP antibody. Quantification of the GFP signal in blots was performed using NIH Image software.

Confocal microscopy. Confocal and time-lapse images were obtained using a Zeiss LSM510 META confocal microscope system (Carl Zeiss, Gottingen, Germany), as described⁴⁹. Images of live cells were acquired using a multi-track setting with line-by-line excitations at 413 nm for CFP and 514 nm for YFP. Appropriate band filters were used to detect both proteins. Fixed cells labelled with antibodies and/or fluorescent proteins were optically sectioned into z-stacks, with the pinhole set to 1 Airy unit. After subtracting background, the average CFP and YFP fluorescence within individual PGCs was quantified in 20 cells per experiment using LSM510-3.2 software and expressed in arbitrary units. Quantification of colocalization between endocytosed anti-Myc antibody and GPI-GFP in polarized MDCK cells was performed in 30–35 cells per experiment using the Colocalization module of LSM510-3.2 software.

Immuno-EM and CVEM analysis. Fixation and immunogold detection of fluorescent proteins for electron microscopy was performed using an anti-GFP antibody as described²⁷. HRP-loaded MDCK cells expressing GPI-YFP were first incubated with the mixture of 0.5 mg/ml di-aminobenzidine (DAB) and 0.01% H_2O_2 in 0.1 M Tris-HCl to detect HRP. Next, GPI-YFP was labelled using the immunogold protocol. After immunolabeling, cells were embedded in Epon-812 and cut into thin sections. CVEM of cells cotransfected with VSV-G-CFP and GPI-Myc-YFP was performed as described⁴⁹. Briefly, transfected COS-7 cells were grown in Petri dishes with CELLocate coverslips (Mat Tek, Ashland, MA). After visualization of fluorescent structures by time-lapse confocal microscopy, cells were fixed, immunolabelled for the Myc tag using the gold-enhance protocol, embedded in Epon-812, and cut into serial sections. A Philips Tecna-12 electron microscope (Philips, Eindhoven, The Netherlands) and ULTRA VIEW CCD digital camera were used to acquire electron microscopy images.

Note: Supplementary Information is available on the Nature Cell Biology website.

ACKNOWLEDGEMENTS

We would like to thank all those who provided us with antibodies and cDNAs; W. Arias, members of the Lippincott-Schwartz lab and the Department of Cell Biology

and Oncology for helpful discussions and critical reading of the manuscript; E.V. Polishchuk for assistance with microinjection; E. Fontana for assistance during manuscript preparation. We acknowledge financial support from the Telethon Italy (grants E.1249 and GFT03006).

COMPETING FINANCIAL INTERESTS

The authors declare that they have no competing financial interests.

Received 21 January 2004; accepted 4 March 2004

Published online at <http://www.nature.com/naturecellbiology>.

- Rodriguez-Boulan, E. & Powell, S. K. Polarity of epithelial and neuronal cells. *Annu. Rev. Cell Biol.* **8**, 395–427 (1992).
- Mostov, K. E., Verges, M. & Altschuler, Y. Membrane traffic in polarized epithelial cells. *Curr. Opin. Cell Biol.* **12**, 483–490 (2000).
- Keller, P. & Simons, K. Post-Golgi biosynthetic trafficking. *J. Cell Sci.* **110**, 3001–3009 (1997).
- Matter, K. & Mellman, I. Mechanisms of cell polarity: sorting and transport in epithelial cells. *Curr. Opin. Cell Biol.* **6**, 545–554 (1994).
- Nelson, W. J. & Yeaman, C. Protein trafficking in the exocytic pathway of polarized epithelial cells. *Trends Cell Biol.* **11**, 483–486 (2001).
- Fiedler, K. & Simons, K. The role of *N*-glycans in the secretory pathway. *Cell* **81**, 309–312 (1995).
- Rodriguez-Boulan, E. & Gonzalez, A. Glycans in post-Golgi apical targeting: sorting signals or structural props? *Trends Cell Biol.* **9**, 291–294 (1999).
- Harder, T. & Simons, K. Caveolae, DLGs, and the dynamics of sphingolipid cholesterol microdomains. *Curr. Opin. Cell Biol.* **9**, 534–542 (1997).
- Simons, K. & Ikonen, E. Functional rafts in cell membranes. *Nature* **387**, 569–572 (1997).
- Casanova, J. E., Apodaca, G. & Mostov, K. E. An autonomous signal for basolateral sorting in the cytoplasmic domain of the polymeric immunoglobulin receptor. *Cell* **66**, 65–75 (1991).
- Hunziker, W., Harter, C., Matter, K. & Mellman, I. Basolateral sorting in MDCK cells requires a distinct cytoplasmic domain determinant. *Cell* **66**, 907–920 (1991).
- Folsch, H., Ohno, H., Bonifacino, J. S. & Mellman, I. A novel clathrin adaptor complex mediates basolateral targeting in polarized epithelial cells. *Cell* **99**, 189–198 (1999).
- Gan, Y., McGraw, T. E. & Rodriguez-Boulan, E. The epithelial-specific adaptor AP1B mediates post-endocytic recycling to the basolateral membrane. *Nature Cell Biol.* **4**, 605–609 (2002).
- Traub, L. M. & Apodaca, G. AP-1B: polarized sorting at the endosome. *Nature Cell Biol.* **5**, 1045–1047 (2003).
- Maier, O., Ait Slimane, T. & Hoekstra, D. Membrane domains and polarized trafficking of sphingolipids. *Semin. Cell Dev. Biol.* **12**, 149–161 (2001).
- Nichols, B. J. *et al.* Rapid cycling of lipid raft markers between the cell surface and Golgi complex. *J. Cell Biol.* **153**, 529–541 (2001).
- Sabharanjak, S., Sharma, P., Parton, R. G. & Mayor, S. GPI-anchored proteins are delivered to recycling endosomes via a distinct cdc42-regulated, clathrin-independent pinocytotic pathway. *Dev. Cell* **2**, 411–423 (2002).
- Slimane, T. A., Trugnan, G. & Van Ijzendoorn, S. C. Hoekstra, D. Raft-mediated trafficking of apical resident proteins occurs in both direct and transcytotic pathways in polarized hepatic cells: role of distinct lipid microdomains. *Mol. Biol. Cell* **14**, 611–624 (2003).
- Hirschberg, K. *et al.* Kinetic analysis of secretory protein traffic and characterization of Golgi to plasma membrane transport intermediates in living cells. *J. Cell Biol.* **143**, 1485–1503 (1998).
- Keller, P., Toomre, D., Diaz, E., White, J. & Simons, K. Multicolour imaging of post-Golgi sorting and trafficking in live cells. *Nature Cell Biol.* **3**, 140–149 (2001).
- Schmoranzner, J., Goulian, M., Axelrod, D. & Simon, S. M. Imaging constitutive exocytosis with total internal reflection fluorescence microscopy. *J. Cell Biol.* **149**, 23–32 (2000).
- Kreitzer, G. *et al.* Three-dimensional analysis of post-Golgi carrier exocytosis in epithelial cells. *Nature Cell Biol.* **5**, 126–136 (2003).
- Kreitzer, G., Marmorstein, A., Okamoto, P., Vallee, R. & Rodriguez-Boulan, E. Kinesin and dynamin are required for post-Golgi transport of a plasma-membrane protein. *Nature Cell Biol.* **2**, 125–127 (2000).
- Ihrke, G. & Hubbard, A. L. Control of vesicle traffic in hepatocytes. *Prog. Liver Dis.* **13**, 63–99 (1995).
- Presley, J. F. *et al.* Dissection of COPI and Arf1 dynamics *in vivo* and role in Golgi membrane transport. *Nature* **417**, 187–193 (2002).
- Matlin, K. S. & Simons, K. Reduced temperature prevents transfer of a membrane glycoprotein to the cell surface but does not prevent terminal glycosylation. *Cell* **34**, 233–243 (1983).
- Polishchuk, R. S. *et al.* Correlative light-electron microscopy reveals the tubular-sacculular ultrastructure of carriers operating between Golgi apparatus and plasma membrane. *J. Cell Biol.* **148**, 45–58 (2000).
- Yeaman, C. *et al.* Protein kinase D regulates basolateral membrane protein exit from *trans*-Golgi network. *Nature Cell Biol.* **6**, 106–112 (2004).
- Barnard, R. J., Morgan, A. & Burgoyne, R. D. Stimulation of NSF ATPase activity by α -SNAP is required for SNARE complex disassembly and exocytosis. *J. Cell Biol.* **139**, 875–883 (1997).
- Low, S. H. *et al.* The SNARE machinery is involved in apical plasma membrane trafficking in MDCK cells. *J. Cell Biol.* **141**, 1503–1513 (1998).
- Newman, T. M., Tian, M. & Gomperts, B. D. Ultrastructural characterization of tannic acid-arrested degradation of permeabilized guinea pig eosinophils stimulated with GTP- γ -S. *Eur. J. Cell Biol.* **70**, 209–220 (1996).
- Brown, D. A., Crise, B. & Rose, J. K. Mechanism of membrane anchoring affects polarized expression of two proteins in MDCK cells. *Science* **245**, 1499–1501 (1989).
- Lisanti, M. P., Caras, I. W., Davitz, M. A. & Rodriguez-Boulan, E. A glycopospholipid membrane anchor acts as an apical targeting signal in polarized epithelial cells. *J. Cell Biol.* **109**, 2145–2156 (1989).
- Brown, D. A. & Rose, J. K. Sorting of GPI-anchored proteins to glycolipid-enriched membrane subdomains during transport to the apical cell surface. *Cell* **68**, 533–544 (1992).
- Fiedler, K., Kobayashi, T., Kurzchalia, T. V. & Simons, K. Glycosphingolipid-enriched, detergent-insoluble complexes in protein sorting in epithelial cells. *Biochemistry* **32**, 6365–6373 (1993).
- Friedrichson, T. & Kurzchalia, T. V. Microdomains of GPI-anchored proteins in living cells revealed by crosslinking. *Nature* **394**, 802–805 (1998).
- Scheiffele, P. *et al.* Caveolin-1 and -2 in the exocytic pathway of MDCK cells. *J. Cell Biol.* **140**, 795–806 (1998).
- Parton, R. G. Caveolae — from ultrastructure to molecular mechanisms. *Nature Rev. Mol. Cell Biol.* **4**, 162–167 (2003).
- Peters, P. J. *et al.* Trafficking of prion proteins through a caveolae-mediated endosomal pathway. *J. Cell Biol.* **162**, 703–717 (2003).
- Mostov, K. E. & Deitcher, D. L. Polymeric immunoglobulin receptor expressed in MDCK cells transcytoses IgA. *Cell* **46**, 613–621 (1986).
- Apodaca, G., Katz, L. A. & Mostov, K. E. Receptor-mediated transcytosis of IgA in MDCK cells is via apical recycling endosomes. *J. Cell Biol.* **125**, 67–86 (1994).
- Zurzolo, C., Lisanti, M. P., Caras, I. W., Nitsch, L. & Rodriguez-Boulan, E. Glycosylphosphatidylinositol-anchored proteins are preferentially targeted to the basolateral surface in Fischer rat thyroid epithelial cells. *J. Cell Biol.* **121**, 1031–1039 (1993).
- Lipardi, C. *et al.* Caveolin transfection results in caveolae formation but not apical sorting of glycosylphosphatidylinositol (GPI)-anchored proteins in epithelial cells. *J. Cell Biol.* **140**, 617–626 (1998).
- Louvard D. Apical membrane aminopeptidase appears at site of cell–cell contact in cultured kidney epithelial cells. *Proc. Natl Acad. Sci. USA* **77**, 4132–4136 (1980).
- Grindstaff, K. K. *et al.* Sec6/8 complex is recruited to cell–cell contacts and specifies transport vesicle delivery to the basal-lateral membrane in epithelial cells. *Cell* **93**, 731–740 (1998).
- Benting, J. H., Rietveld, A. G. & Simons, K. *N*-Glycans mediate the apical sorting of a GPI-anchored, raft-associated protein in Madin-Darby canine kidney cells. *J. Cell Biol.* **146**, 313–320 (1999).
- Pang, S., Urquhart, P. & Hooper, N. M. *N*-Glycans, not the GPI anchor, mediate the apical targeting of a naturally glycosylated, GPI-anchored protein in polarised epithelial cells. *J. Cell Sci.* (in the press).
- Yeaman, C. *et al.* The *O*-glycosylated stalk domain is required for apical sorting of neurotrophin receptors in polarized MDCK cells. *J. Cell Biol.* **139**, 929–940 (1997).
- Polishchuk, E. V., Di Pentima, A., Luini, A. & Polishchuk, R. S. Mechanism of constitutive export from the Golgi: bulk flow via the formation, protrusion, and *en bloc* cleavage of large *trans*-Golgi network tubular domains. *Mol. Biol. Cell* **14**, 4470–4485 (2003).
- Rodriguez-Boulan, E. *et al.* Methods to estimate the polarized distribution of surface antigens in cultured epithelial cells. *Methods Cell Biol.* **32**, 37–56 (1989).